

## ICON28-POWER2020-16562

### MELCOR VALIDATION STUDY ON MULTI-ROOM FIRE

**David L.Y. Louie<sup>1</sup>**  
Sandia National Laboratories  
Albuquerque, New Mexico, USA

**Samir El-Darazi<sup>2</sup>, Lyndsey M. Fyffe, James L. Clark**  
Los Alamos National Laboratory  
Los Alamos, New Mexico, USA

#### ABSTRACT

*Estimation of radionuclide aerosol release as a source term (ST) to the environment from fire scenarios are one of the most dominant accident evaluations at the U.S. Department of Energy's (DOE's) nuclear facilities. Of particular interest to safety analysts is estimating Source Term (ST) based on aerosol transport from a fire room to a corridor and from the corridor to the environment. However, no existing literature has been found on estimating ST from this multi-room facility configuration. This paper contributes the following to aerosol transport modeling body of work: a validation study on a multiroom fire experiment (this includes a code-to-code comparison between MELCOR and Consolidated Fire and Smoke Transport, a specialized fire code without radionuclide transport capabilities), a sensitivity study to provide insight on the effect of smoke on ST, and a sensitivity study on the effect of aerosol entrainment in the atmosphere (puff and continuous rate) on ST.*

Keywords: MELCOR, fire, aerosol transport, source term, leak path factor

#### NOMENCLATURE

BR	Burn (fire) Room
CCF	Counter Current Flow
CF	Control Function
CR	Corridor
CV	Control volume
DOE	U.S. Department of Energy
HRR	Heat Release Rate
LANL	Los Alamos National Laboratory
LPF	Leak Path Factor
RN	Radionuclide
s	Smoke
Sandia	Sandia National Laboratories
ST	Source Term

TR	Target room
u	$UO_2$
$C_D$	Discharge coefficient
$\Delta\rho$	Density ( $\rho$ ) difference
l	Characteristic length
$Q_{cc}$	Volumetric flow
$X_{cc}$	Coefficient defined in Equation (2)

#### 1. INTRODUCTION

Fire accidents are the most dominant accident condition at the U.S. Department of Energy's (DOE's) nuclear facilities, including those at Los Alamos National Laboratory (LANL). When a fire occurs in a facility with radioactive materials, such as plutonium dioxide ( $PuO_2$ ), the transport of  $PuO_2$  through pathways within the facility, leading to release from the facility is called "leak path.". The fractional release due to this leak path is called the leak path factor (LPF). Traditionally, an LPF is calculated using the DOE toolbox code [1]—MELCOR. [2]. MELCOR is a system-level code developed at Sandia National Laboratories (Sandia) for the U.S. Nuclear Regulatory Commission.

As a part of LPF guidance for using MELCOR, a recent study concluded that MELCOR can be used to model a fire scenario to capture the thermal-hydraulic condition of a fire in a volume well. [4]. However, that study did not include the multi-room effects that typically occur in many facilities where a fire starts in an inner room and propagates through a corridor and then to the environment via door gaps or open doors.

Specifically, the following contributions were made by using MELCOR code [2]: a validation study on the FM21 multi-room fire experiment [6] (this includes a code-to-code comparison between MELCOR and Consolidated Fire and Smoke Transport (CFAST), [3] a specialized fire code without aerosol transport capabilities), a sensitivity study to provide insight on the effect of smoke on ST, and a sensitivity study on

<sup>1</sup> Contact author: dllouie@sandia.gov

<sup>2</sup> Los Alamos National Laboratory-Environmental Management

the effect of aerosol entrainment rates to the atmosphere (puff and continuous rate) on ST.

This paper is organized as follows: First, we describe the multi-room fire experiment (FM21). Second, we describe the aerosol treatment for smoke and the contaminant ( $UO_2$  for  $PuO_2$ ) in MELCOR. Third, we present the MELCOR model setup that was used to validate thermal hydraulic and smoke transport from the FM21 test. The results section presents a discussion on the FM21 validation, the effects of smoke on ST, and the effect of contaminant entrainment rate on ST as well. Last, insights gained from the study are summarized in the conclusion.

## 2. MULTIROOM FIRE EXPERIMENT

A recent MELCOR guidance study on fire modeling indicates that MELCOR can be used to model fire, even though MELCOR does not contain a dynamic hot gas layer as in CFAST. [4]. Modeling fire using MELCOR is described later in this paper. For MELCOR fire validation, a multiroom configuration with a corridor fire and smoke experiment that is documented in the CFAST validation report [5] was used. This experiment (FM21) was one of the 60 fire experiments conducted in a facility at the Factory Mutual Research Corporation factory in 1985. [6]. The FM21 test is briefly described in the following subsection. followed by a section to describe the aerosol treatment when considering more than one aerosol (such as soot and a heavy contaminant), because MELCOR requires these inputs.

The multiroom fire experiment (FM21) was conducted inside a  $67\text{ m} \times 76\text{ m} \times 18.3\text{ m}$  facility [6], shown in FIGURE 1. The facility includes a Burn Room (BR) where the fire source (burner) is located and an 18.9 m Corridor (CR) connected to Target Rooms (TR) with doorways. All interior doors were always open. A 12.7 mm thick gypsum board on wood studs was used throughout the enclosure, except for the BR, which was walled with special material to harden against repeated fire exposure. All flooring was made of concrete. A fire burner (0.91 m diameter and 0.58 m high) in BR is shown as a red dot. Propylene fuel was selected because of its high yield of smoke that is easily traceable by eye and the optical devices (photometers). In this test, there was no active ventilation and no environment flow effects because the external window/door connections were closed. Many measurements and sensor arrays were placed in the enclosure, including thermocouples, photometers, flow probes, turbidimeters, and wall pressure gauges. The raw experimental data were obtained from [7], which was also used for the CFAST validation [3].

## 3. AEROSOL TREATMENT

As indicated in Section 2, only smoke was qualitatively collected in the FM21 test. It is difficult to interpret the results into quantitative data that can be correlated to use in modeling as aerosol. To model an ST release from a fire, a minimum of two aerosol sources is required. The first aerosol is the smoke (or soot), which is a by-product of a fire. Most of the combustibles encountered at DOE facilities are carbon-based combustibles. Therefore, the soot is a carbon-chain material that is light-weight

and tends to be a non-spherical shape. The other aerosol modeled is usually the contaminant (e.g.,  $PuO_2$ ) for ST. First, we discuss the aerosol of the smoke for the propylene. Then the release method of the ST aerosol,  $UO_2$  for  $PuO_2$  is given, because  $UO_2$  data is widely available.

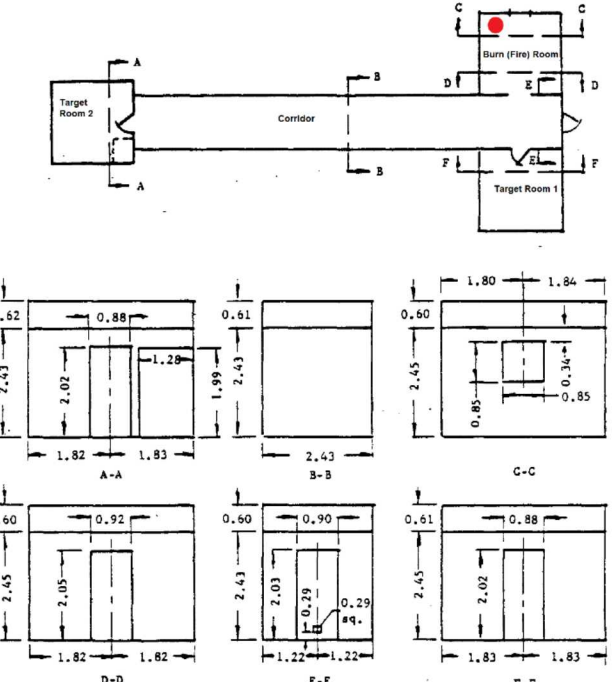


**FIGURE 1: MULTI-ROOM ENCLOSURE DIMENSION (IN METERS) [6]. THE RED DOT REPRESENTS THE LOCATION OF THE BURNER**

### 3.1. Smoke Data

While FM21 smoke data was measured qualitatively, a quantity value associated with this fuel material was needed. Based on [8], smoke characteristics from the propylene burner were not provided in the FM21 test. Hence, the smoke characteristics for this study were obtained from [8], using a smoke production rate of 0.095 gram of smoke per gram of fuel. The aerodynamic diameter of  $0.15\text{ }\mu\text{m}$  with a geometric standard deviation of 2 and a molecular weight of 42 g/mole was used. In general, the soot particle in a carbon/hydrogen chains may have a density between 1 to 2 g/cc. However, because the smoke particles are not spherical, they tend to have an aerodynamic shape factor much larger than 1. Thus, a 0.8 g/cc density is assumed for this smoke aerosol.

### 3.2. Contaminant Data

For the contaminant, we model  $UO_2$  for representing plutonium oxide materials. [9]. Unlike the smoke particles, which can have a non-spherical shape, the plutonium oxide or  $UO_2$  is typically ball milled into small particles that could have a shape closely configured into a spherical shape. When the  $UO_2$  aerosols are agglomerated, they may exhibit a spherical shape.  $UO_2$  aerosol data is given in TABLE 1.

**TABLE 1: DERIVED UO<sub>2</sub> MASS/SIZE DISTRIBUTION [4]**

Bin #	Diameter (μm)	Mass Fraction
1	0.1-0.186	0.008
2	0.186-0.347	0.051
3	0.347-0.645	0.100
4	0.645-1.20	0.108
5	1.20-2.24	0.162
6	2.24-4.16	0.162
7	4.16-7.75	0.108
8	7.75-14.4	0.108
9	14.4-26.9	0.086
10	26.9-50.0	0.108

Unlike the release of smoke in a fire, which can be proportional to the fire curve, the contaminant release is greatly dependant on the accident scenario. For example, if a fire is driven by the burning of a contaminated paper towel with a uniformly distributed contaminant, then the release may be proportional to the fire curve. However, in a seismic event that includes a radionuclide contaminant spill followed by a fire, the release of the contaminant occurs instantaneously. The timing of the release and the start of the fire may be important to determine the attenuation of the suspended particles. The following two approaches are used in the MELCOR model to model these diverse release dynamics:

*Approach A* (continuous release) is that the release follows the fire curve—simulating a uniformly contaminated combustible solid. As a rule of thumb, any particle size  $\leq 10$  μm is considered respirable, which means that the particle tends to stay suspended in air while larger aerosols would eventually settle.

*Approach B* (puff release) is an instantaneous release at the start of the fire, which simulates a contaminated spill immediately followed by a fire. MELCOR treats aerosols as trace particles. To model the spill without of prescribed ventilation flow (i.e., from the heating, ventilation, and air conditioning system), an estimate of the induced air flow may be required. The magnitude of the induced flow may be small in comparison to the internal natural circulation flows. [4]

#### 4. MELCOR MODEL

MELCOR (Version 2.2.9541) was used in this study. Detailed information on MELCOR user input and its associated physics packages is documented in [2].

In this validation study, four areas of focus are observed: 1) validate the thermal-hydraulic behavior of the fire in the experiment by modeling the fire combustion, 2) simulate the hot gas layer buildup in the burn room by dividing the room into three horizontal control volumes (CVs) and then capture the fire area in the corner of the room (in two vertical segments), 3) apply the countercurrent flow model within MELCOR to model the recirculating flow of the hot and cold air exchange in the doorway at the bottom of two horizontal volumes, and 4)

simulate the smoke tendency to rise in the upper portion of the room until the hot gas layer expands to the doorway where a horizontal CV is added to the top of the doorway.

To achieve the fire phenomenology described above, the MELCOR model representation of FM21 is shown in FIGURE 2. As shown in this figure, the BR is labeled as Compartment 1 and modeled with six CVs. A corner area consists of a fire source using three horizontal CVs to allow stratification (CV10x). Outside of the corner area within the BR are the three horizontal CVs. A total of six CVs represents the BR. The fire source starts at the bottom-most CV (CV101). MELCOR contains a countercurrent flow model (CCF) that predicts the hot and cold exchange through the doorway.

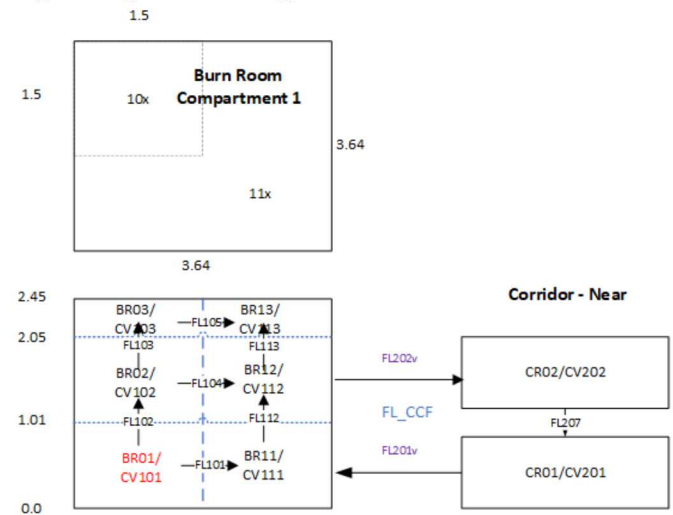


**FIGURE 2: NODALIZATION OF BR AND CR GEOMETRY REPRESENTATION AND FLOW PATHS (IN METERS)**

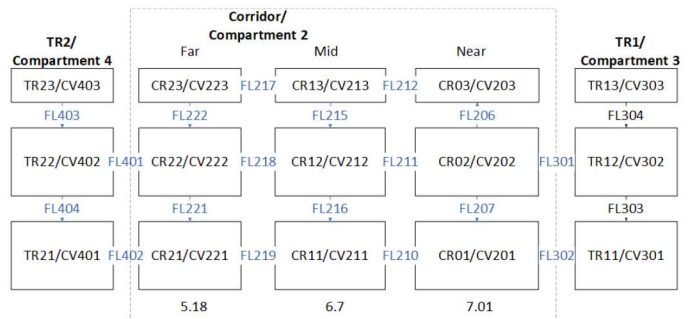


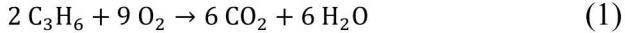
**FIGURE 3: NODALIZATION OF MELCOR REPRESENTATION OF FM21 CR AND TR1/TR2 GEOMETRY (IN METERS)**

Similarly, the corridor and the connected target rooms (TR1 and TR2) are also represented by three horizontal CVs (see FIGURE 3). For the corridor, there are three segments: near, middle, and far indicating the region close to the BR versus the region closer to TR2. The compartment number in the nodalization is compared to CFAST data. [3] In this MELCOR model, only a single CCF model is used between the corridor and BR air exchange. Because the FM21 test does not model the environment outside the enclosure for gas and smoke releases,

the releases from the FM21 experiment goes into a time-independent control volume for the environment (see [2] for details).

#### 4.1. Fire Model

The measured heat release rate (HRR) of the propylene fire was 522 kW. The associated fire reaction Equation (1) was modeled according to the experimental report, [6] with a specific reaction heat (SRH) of 45,800 kJ/kg.



Consequently, the steady state fuel consumption rate can be calculated as HRR/SRH, or 0.0114 kg/s. Using this consumption rate, the reactant consumption rates and product generation rates are calculated and modeled in MELCOR using the control functions (CFs) package inputs (i.e., mass and energy sinks/sources). The use of CFs to model fire is described in the guidance report. [4]. The fire power history for FM21 including both the growth, steady, and decay phases was not available. Consequently, the MELCOR fire history was specified using the same assumptions from the CFAST FM21 input deck (see the normalized fire curve from CFAST in FIGURE 4). [10]. As shown in FIGURE 4, the fire starts at about 180 s. The assumed fraction of the energy from the fire radiated to the surfaces of the BR is 33% (i.e., same assumptions as the CFAST FM21 model).

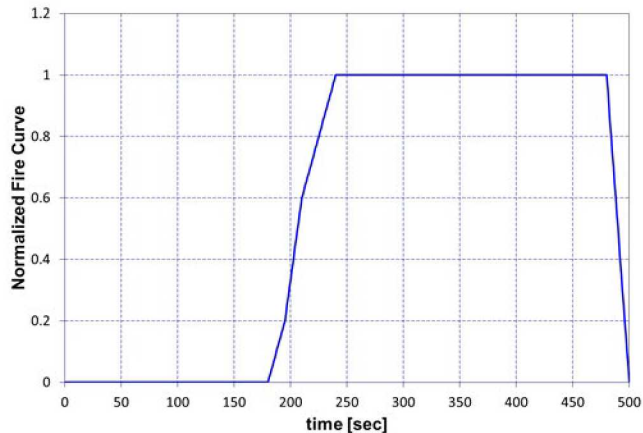


**FIGURE 4: NORMALIZED FIRE CURVE USED IN MELCOR**

In MELCOR, each surface in BR will receive the fraction of the fire energy based on its surface area divided by the total surface area in the room. Because the FM21 data did not include any specification of heat structures such as walls, ceilings, and floors, the CFAST structural input data was used, such as flooring made of concrete with a thickness of 0.15 m. The walls and ceilings are made of gypsum board at 0.5 in (1.27 cm) thick. The gypsum thermophysical properties from CFAST were also used (i.e., the heat capacity of 0.9 kJ/kg-C and density of 790 kg/m<sup>3</sup>). The CFAST thermal conductivity of 0.16 kW/m-C was 100 times larger than the value found in the open literature. In addition, we assume that the external surfaces of walls and ceilings are connected with the environment. The floors were

assumed to be adiabatic. The door structures and wood frames were not modeled.

The MELCOR fire model included the consumption of O<sub>2</sub> and production of CO<sub>2</sub> and H<sub>2</sub>O according to Equation (1) reaction because the measurement data is available. For the initial conditions of the rooms and the corridor, a humidity of 0.5, temperature of 288 K, and 0.206 O<sub>2</sub> and 0.795 N<sub>2</sub> air mole fractions were used. Note, CFAST used an initial O<sub>2</sub> mole fraction of 0.2165.

#### 4.2. CCF Model

Countercurrent flow between the fire room and corridor is a well understood phenomenon. [11] Although MELCOR is limited with fixed control volume boundaries, it can account for CCF exchange between the fire room and corridor by using the CCF model. [4]. This horizontal CCF model is represented in the following equation as:

$$Q_{cc} = X_{cc} C_D \sqrt{\frac{l^5 g \Delta \rho}{\bar{\rho}}} \quad (2)$$

where Q<sub>cc</sub>=volumetric flow of pure countercurrent flow (m<sup>3</sup>/s), X<sub>cc</sub>=a coefficient, which is a function of the orientation and geometry of the opening, such as square versus round, C<sub>D</sub>=discharge coefficient, l=characteristic dimension such as the opening height (m), g= gravity (m<sup>2</sup>/s), Δρ=density difference (kg/m<sup>3</sup>), and  $\bar{\rho}$ =average density (kg/m<sup>3</sup>). For a rectangle doorway, X<sub>cc</sub>=0.3333 is recommended. For a perfect exchange of flow in a doorway, the upper flow (generally hot) should be equal to the lower flow (generally cold). Thus, the net flow should be zero. As shown in the above equation, C<sub>D</sub> increases with an increasing flow. Note that the magnitude of the CCF flow is a function of the donor (or upstream) density.

#### 4.3. Aerosol Model

Using the assumptions of the aerosol treatment in Section 3, both smoke (according to Section 3.1) data and contaminant data (in this case, use UO<sub>2</sub> data and input according to TABLE 1) are added to the MELCOR model for the soot accumulation and contaminant transport. Because smoke is not a default class in the Radionuclide package within MELCOR, a new class was added. Currently, MELCOR only allows a single density for all aerosols. In this case where both low-density soot and high-density contaminant aerosols exist; the use of the larger density may yield a better result. A sensitivity study on the effect of the density is provided. For the release of contaminant, continuous (follows the fire curve, see FIGURE 4) and puff releases (see FIGURE 5) are also considered.

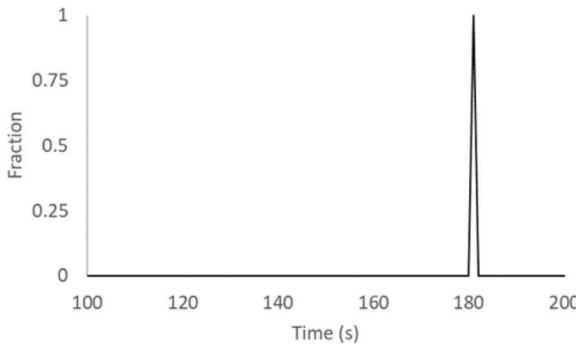


**FIGURE 5** PUFF RELEASE TO SIMULATE SPILL

## 5. RESULTS AND DISCUSSION

This section discusses the results of MELCOR cases to simulate the FM21 test. The thermal-hydraulic results as shown in Section 5.1 and the sensitivity studies on the effect of the smoke and  $UO_2$  aerosol transport alone are discussed in Section 5.2, which includes sensitivity studies on the effect on ST based on the aerosol formation modeling (i.e., continuous versus a puff source) and use of time independent environmental volumes. The MELCOR results are compared to both experimental and CFAST data provided in [7], as appropriate.

### 5.1 Thermal-Hydraulic Behavior

This section discusses the thermal-hydraulic results used to validate the MELCOR model for BR (described in Section 4.1) against the experimental data in Section 2. Four cases, shown in TABLE 2, were used to iteratively tune the model to agree with experimental data for the fire curve shown in FIGURE 4. Ultimately Case 0 was selected to be best suited for the aerosol study as described in Section 3, based on the observations of all cases discussed in this section.

**TABLE 2:** MELCOR CASES FOR THE THERMAL-HYDRAULIC STUDY

Case	Description	Comments
0	Use CCF ( $C_d=0.5$ ). Fraction of fire heat loss, $H_{loss}$ to heat structures is set at 33% same as CFAST.	Establishes the tuned thermal-hydraulic model before conducting aerosol simulations.
1	Same as Case 0, but $H_{loss}$ is assumed to 50%.	Attempts to match temperatures and pressure in BR by increasing $H_{loss}$
2	Same as Case 0, except increases $C_d=0.75$	This case attempts to match pressure between BR and CR by increasing the $C_d$
3	Same as Case 0, except increases $C_d=0.25$	Attempts to match pressure between BR and CR by decreasing $C_d$

As shown in FIGURE 6 for Case 0, the production and consumption of the gases according Equation (1) follows the fire curve (see Fig. 4). Using the HRR in FM21 with the fire curve, the power produced during the fire is given in FIGURE 7. The consumption of  $O_2$  and fuel produces both  $CO_2$  and  $H_2O$ . FIGURE 8 shows the MELCOR results for Case 0 on the  $O_2$  mole fractions in BR. As shown in FIGURE 8, the MELCOR

predictions are in line with the experimental data (i.e., the CFAST results are included for comparison). Note that CFAST predicts slightly lower oxygen decrease than the experimental data. As shown in FIGURE 9, MELCOR closely follows the experimental data for  $CO_2$  mole fraction in BR. Both MELCOR and CFAST overpredicted the  $CO_2$  production in comparison to the experimental data. FIGURE 10 shows the comparison of MELCOR results for BR gas temperatures to both CFAST and experimental data. The gas temperatures predicted by MELCOR is within the range of the data and CFAST. The temperature at the bottom layer of BR obtained from MELCOR is due the gas inflow from the corridor, which is cooler. These figures demonstrate that using CFs in MELCOR can model chemical reactions of a fire in both gas composition and fire energy adequately.

To observe the effect of heat loss to surfaces, we compare Case 0 with Case 1. As shown in FIGURE 11, increased heat loss reduced the countercurrent flow to all doorways. This is caused by the temperature-induced pressure being lower for the case with increased heat loss (see BR gas temperatures and pressures comparison in FIGURE 12 and FIGURE 13, respectively).

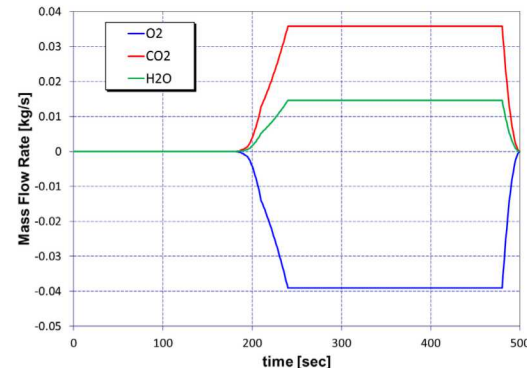


**FIGURE 6:** GAS FLOW RATES DURING FIRE FOR CASE 0

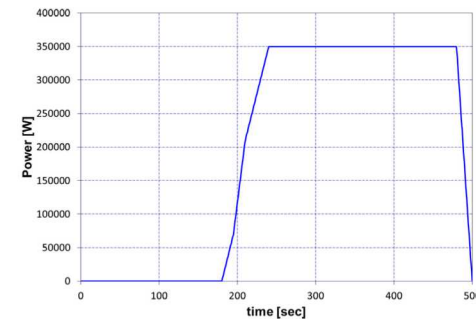


**FIGURE 7:** FIRE ENERGY RATE FOR CASE 0

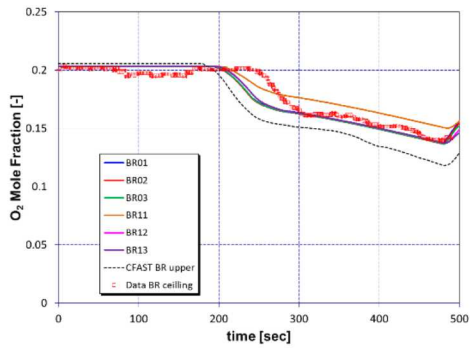


**FIGURE 8:** BR O<sub>2</sub> MOLE FRACTIONS FOR CASE 0

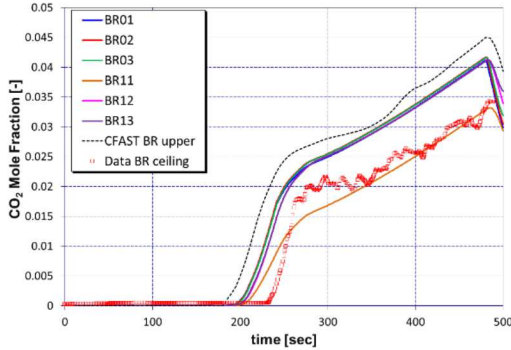


**FIGURE 9:** BR CO<sub>2</sub> MOLE FRACTIONS FOR CASE 0

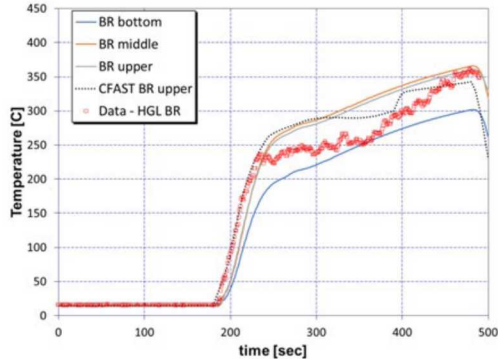


**FIGURE 10:** BR GAS TEMPERATURES FOR CASE 0

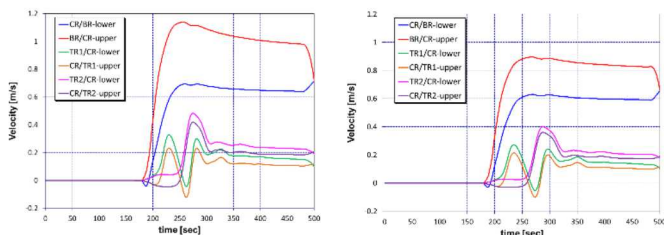


**FIGURE 11:** COMPARISON BETWEEN CASES 0 AND 1 ON GAS VELOCITIES AT THE DOORWAYS

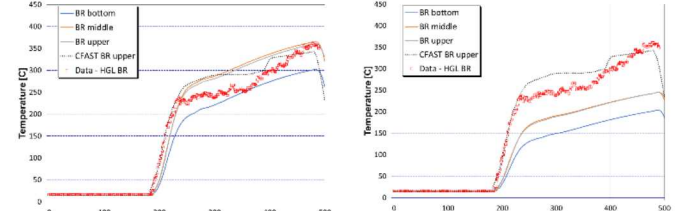


**FIGURE 12:** COMPARISON BETWEEN CASES 0 AND 1 ON BR GAS TEMPERATURES

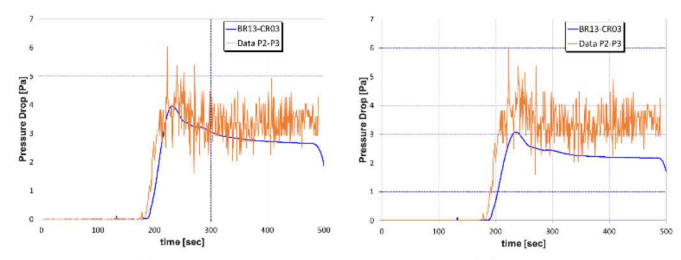


**FIGURE 13:** COMPARISON BETWEEN CASES 0 AND 1 ON GAS PRESSURE DROP ACROSS BR AND CR DOORWAY

Another sensitivity study is observing the effect of the drag coefficient ( $C_D$ ) in the CCF model in MELCOR as shown in Equation (2). As shown in FIGURE 14, increasing  $C_D$  (Case 3) will result higher flow velocities at the doorways, and decreasing  $C_D$  (Case 2) will result in lower flow velocities at the doorways. These changes would affect the gas pressure drop across the BR and CR as shown in FIGURE 15. As shown in this figure, increasing flow velocity would increase pressure drop, while decreasing flow velocity would decrease pressure drop.

As shown in FIGURE 16 for the gas temperature comparison in BR, the best case for matching the experimental data is Case 0 with  $C_D$  of 0.5, even though the pressure drop at the end of the simulation is slightly lower than the data. The next section describes the aerosol transport results using Case 0.

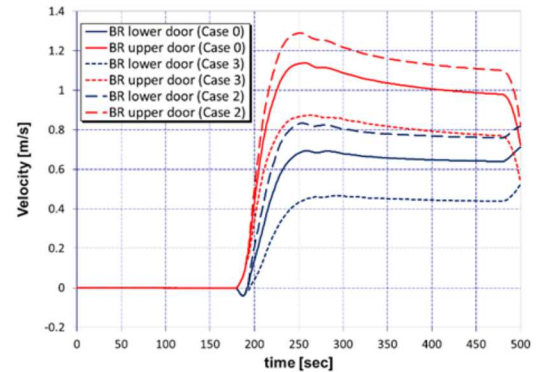


**FIGURE 14:** COMPARISON OF BR GAS VELOCITIES FOR CASES 0, 2 AND 3 ON  $C_D$

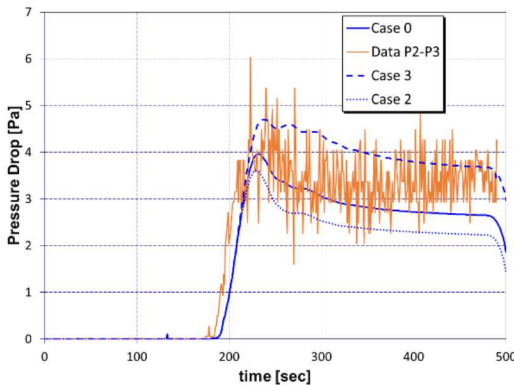


**FIGURE 15:** COMPARISON OF BR GAS PRESSURE ACROSS BR AND CR DOORWAY

As shown in FIGURE 16 for the gas temperature comparison in BR, the best case for matching the experimental data is Case 0 with  $C_D$  of 0.5, even though the pressure drop at the end of the simulation is slightly lower than the data. The next section describes the aerosol transport results using Case 0.

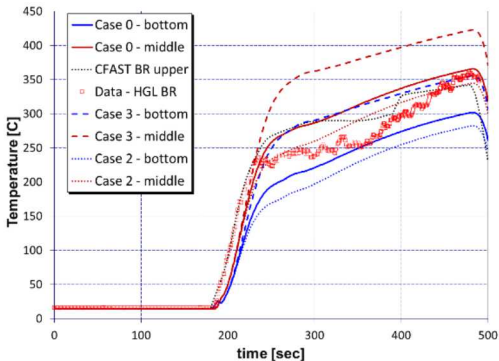


**FIGURE 16:** BR GAS TEMPERATURES OF CASES 0, 2 AND 3

## 5.2 Aerosol Transport Behavior

In this section, the sensitivity study of aerosol transport (smoke and  $UO_2$ ) is described. TABLE 3 lists three major case sets conducted for 1) smoke only, 2)  $UO_2$  only, and 3) combined smoke and  $UO_2$ . In the last set of sensitivity calculations, the treatment of environment connections to the FM21 facility is varied. The corridor connected to the burn or fire room may be located adjacent to an external door where release is possible.

As shown in Table 3, the modeling affecting the aerosol characteristics is varied to identify the range of results, since MELCOR currently allows to model only a single aerosol density for all components (such as smoke and  $UO_2$ ). Using a lighter density, such as the smoke may result a larger release while using a heavier density, such as  $UO_2$  may result a smaller release.

A comparison of MELCOR (Case 4) and experimental relative smoke concentration is shown in FIGURE 17 and FIGURE 18 for the photodetectors located in the corridor near the burn room, and mid-section corridor length from the burn room, respectively. As shown in these figures, with the exception

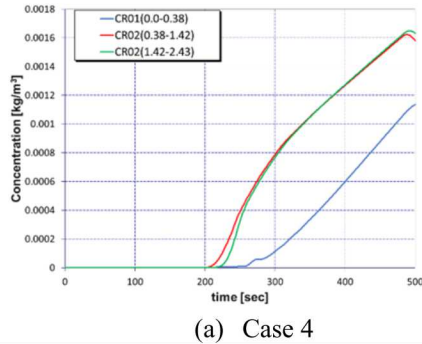
of the CR-near location, MELCOR has the same trend as the experimental data (i.e., the smoke concentration is highest near the ceiling, then diminishes downward).

**TABLE 3:** MELCOR CASES FOR THE AEROSOL TRANSPORT STUDY

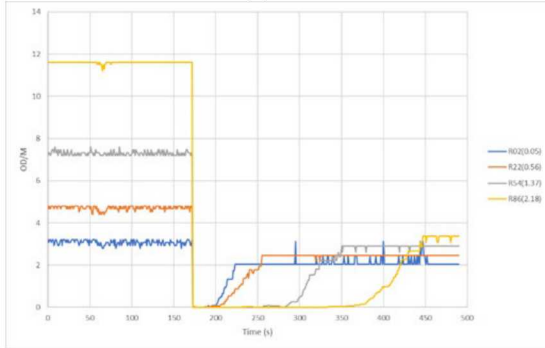
Case	Description	Comment
<b>Smoke only</b>		
4	Add smoke data as a continuous release with 0.29 kg total to Case 0 according to Section 5.1.	As a baseline case for smoke transport only
5	Same as Case 4, except aerosol density set to 11000 kg/m <sup>3</sup>	Since smoke is light, assume its density to $UO_2$
6	Same as Case 4, except increased the total smoke mass to ~1kg	Increase smoke mass to 1 kg from 0.29 kg
7	Same as Case 6, except use a density of 11000 kg/m <sup>3</sup>	Increase both density and mass of smoke
<b><math>UO_2</math> only</b>		
8	Add $UO_2$ data to Case 0 using approach A with a total mass of 100 g	As a baseline case for $UO_2$ transport only (Table 1)
8a	Same as Case 8 but use a single size source at bin 8 (see Table 1)	Using Case 8, but source in a single bin 8 only.
9	Same as Case 8, except aerosol density set to smoke density of 800 kg/m <sup>3</sup>	Using Case 8, but use smoke density
9a	Same as Case 9, except use a single size source at bin 10 due to the density difference between $UO_2$ and smoke	Using Case 9, source in a single bin 10 only with smoke density
9b	Same as Case 9a, except single source at bin 8	Same as Case 9a, except source to single bin 8.
9c	Same as Case 9b, except using a weighted density (3406.7 kg/m <sup>3</sup> )	Examine effect of a mass weighted density between smoke and $UO_2$
10	Same as Case 8, but using approach B	Instead of continuous, use puff release
11	Same as Case 10, except aerosol density set to smoke density of 800 kg/m <sup>3</sup>	Examine density effect on puff release
<b>Smoke and <math>UO_2</math></b>		
12	Combining Case 5 and Case 8: in continuous release, aerosol density set to 11000 kg/m <sup>3</sup>	Effect of 2 aerosols (smoke and $UO_2$ ) in continuous release with $UO_2$ density
13	Same as Case 12, except set to smoke density of 800 kg/m <sup>3</sup>	Use smoke density, continuous release
14	Combining Case 5 and Case 10: puff release for $UO_2$ , using aerosol density set to 11000 kg/m <sup>3</sup>	Use puff release for $UO_2$ and its density for aerosol
15	Same as Case 14, except set to smoke density of 800 kg/m <sup>3</sup>	Use puff release for $UO_2$ and smoke density for aerosol
16	Same as Case 12, except using a weighted aerosol density of 3406.7* kg/m <sup>3</sup>	Continuous release with mass weighted density between smoke and $UO_2$
17	Same as Case 15, except set to weighted density of 3406.7 kg/m <sup>3</sup>	Puff release with mass weighted density between smoke and $UO_2$
<b>Smoke and <math>UO_2</math>, but treat TR1 and TR2 as time independent volumes</b>		
18	Same as Case 15, except set TR1 and TR2 as time-independent CVs	Treatment of TR1 and TR2 as constant temperature and pressure volumes

Case	Description	Comment
19	Same as Case 17, except set TR1 and TR2 as time-independent CVs	Treatment of TR1 and TR2 as constant temperature and pressure volumes
20	Same as Case 18, except use $\text{UO}_2$ density	Treatment of TR1 and TR2 as constant temperature and pressure volumes
21	Same as Case 19, except use $\text{UO}_2$ density	Treatment of TR1 and TR2 as constant temperature and pressure volumes

\*Mass averaged density assumed 0.29 kg smoke and 0.1 kg  $\text{UO}_2$



(a) Case 4



(b) Experimental data

**FIGURE 17:** SMOKE TREND COMPARISON FOR CR-NEAR LOCATIONS

For the cases with only smoke aerosols, TABLE 4 shows the aerosols results of four cases conducted using MELCOR in terms of aerosol fraction. As shown in this table, an increased aerosol density will decrease the amount of aerosol suspended at the end of the test. An increased initial smoke mass will also increase the amount suspended in fractional values. The results are expected since gravitational force is higher for higher density material. High mass translated into more aerosols, which encourage agglomeration to occur, allowing the larger aerosol to settle.

**TABLE 4:** MELCOR CASES FOR THE SMOKE TRANSPORT ONLY

Case	Aerosol initial mass (kg)	Release	Density (kg/m³)	Aerosol Fraction*	
				Atmos.	Dep.
4	0.29	Continuous	800.0	0.9313	0.0687
5	0.29	Continuous	11000.0	0.9221	0.0779
6	1.0	Continuous	800.0	0.9357	0.0643
7	1.0	Continuous	11000.0	0.9266	0.0734

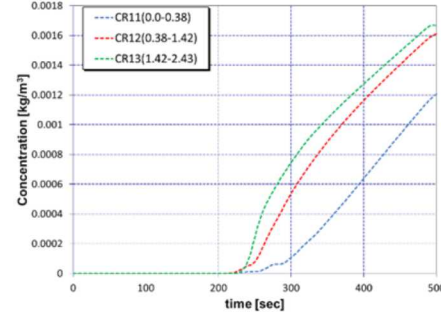
\*at the end 500 s simulation time

In terms of  $\text{UO}_2$  aerosol only simulations, TABLE 5 shows the effect of continuous and puff releases, and density changes. Both Case 8 and 9 models have similar fire and smoke transport and deposition characteristics, but Case 8 uses the  $\text{UO}_2$  density while Case 9 uses the smoke density with the same particle distributions (see TABLE 1). FIGURE 19 and FIGURE 20 show the  $\text{UO}_2$  aerosol airborne concentration and deposition mechanisms for Cases 8 and 9, respectively. Case 8 has a lower airborne fraction than Case 9 as shown in FIGURE 19, which is due to the density difference (density in Case 8 is 14 times higher than that of Case 9). The results show the gravitational settling 4 times higher in Case 8 than Case 9 as shown in FIGURE 20.

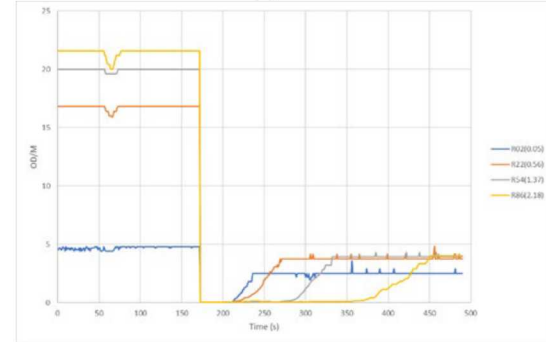
**TABLE 5.** MELCOR CASES FOR THE  $\text{UO}_2$  TRANSPORT ONLY

Case	Aerosol Dist.	Release	Density (kg/m³)	Aerosol Fraction*	
				Atmos.	Dep.
8	Table 1	Continuous	11000.0	0.6186	0.3814
8a	Bin 8	Continuous	11000.0	0.2138	0.7862
9	Table 1	Continuous	800.0	0.8275	0.1725
9a	Bin 10	Continuous	800.0	0.2496	0.7504
9b	Bin 8	Continuous	800.0	0.8524	0.1476
9c	Table 1	Continuous	3407.0	0.5556	0.4444
10	Table 1	Puff	3407.0	0.4886	0.5114
11	Table 1	Puff	800.0	0.7193	0.2807

\*at the end 500 s simulation time



(1) Case 4



(2) Experimental data

**FIGURE 18:** SMOKE TREND COMPARISON FOR CR-MIDDLE LOCATIONS

If the smoke density is used instead of the heavier  $\text{UO}_2$  density, the gravitational settling is similar. However, if the particle size is larger, it should settle faster as described in Section 3.1. To test this, the initial aerosol size is specified for one size bin (i.e., Bin 8) instead of a mean size with a standard

deviation. Case 8a modifies Case 8 by assuming that all aerosol is sourced in Bin 8 (7.75-14.4  $\mu\text{m}$ ). To model the same settling effect, the particle size needs to be increased if the smoke density is used. In this case, Bin 10 is used (26.9-50.0  $\mu\text{m}$ ) for Case 9a. To confirm the results in Case 9a, where the aerosol diameter has been adjusted due to the use of a lighter density, Case 9b uses the same lighter smoke density but it assumes all aerosol in Bin 8. The deposited mass fraction decreased to 0.1476, which confirmed what is needed to yield similar results as Case 9. This helps substantiate the results between Case 8a and 9a. A weighed density approach as shown in Case 9c yields a better result if the particle size adjustment is not used. These simulation results indicate that to compensate the effect of density, a particle size adjustment is a preferred method when using a very different density.

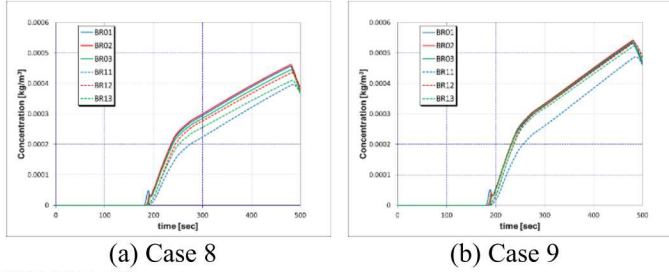


**FIGURE 19:** UO<sub>2</sub> AIRBORNE CONCENTRATIONS IN BR FOR CASES 8 AND 9

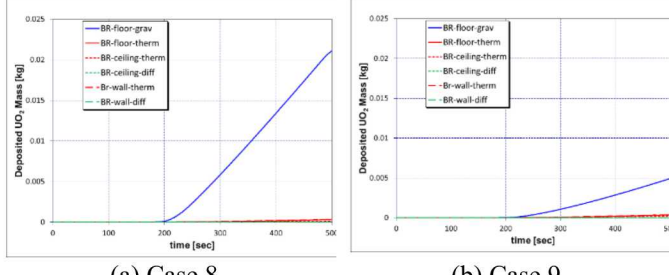


**FIGURE 20:** UO<sub>2</sub> DEPOSITIONS IN BR FOR CASES 8 AND 9

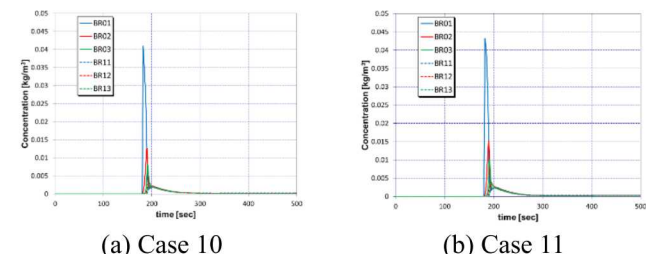


**FIGURE 21:** UO<sub>2</sub> IN AIR IN BR FOR CASES 10 AND 11

To model the initial puff of UO<sub>2</sub> at the start of the fire to simulate the release followed by fire (see FIGURE 5), Cases 10 and 11 use this approach but with a density of UO<sub>2</sub> and smoke, respectively. FIGURE 21 (a) and (b) show the comparison of the density effect for Cases 10 and Case 11, respectively. The heavier UO<sub>2</sub> density has a lower airborne concentration compared to the lighter smoke density. FIGURE 22 illustrates this trend and the comparison on the deposition mechanism, which is primarily

gravitational settling. Decreasing the density by a factor of 14 decreases the gravitational settling by a factor of three in the BR during this fire scenario.

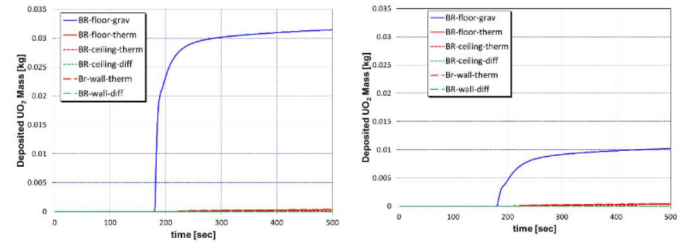


**FIGURE 22:** UO<sub>2</sub> DEPOSITION IN BR FOR CASES 10 AND 11

The previous results have used a single aerosol definition. Combining lighter and heavy aerosols in a simulation requires use of an appropriate representative density. TABLE 6 shows the MELCOR results for the combination of two aerosols using smoke, UO<sub>2</sub> and mass weighted density. As shown in TABLE 6, the results for Cases 12 and 13 seem to agree well with the individual aerosol study for the smoke (Cases 4 and 5 in TABLE 4) and for UO<sub>2</sub> (Cases 8 and 9 in TABLE 5) for approach A. The findings of using approach B (Case 14 and 15) show close results to approach A (Case 12 and 13), which means that the effect of smoke onto the UO<sub>2</sub> release may not be significant. It is suspected that the smoke-contaminant ratio of 0.29 kg per 0.1 kg may be too small to have any effect on UO<sub>2</sub> release. In comparison to a previous study on smoke in Appendix A.2 of [4], 1 g of UO<sub>2</sub> per 0 kg, 10kg, and 25 kg of smoke decreased the from 0.0030, 0.0027, and 0.0024, respectively.

**TABLE 6:** MELCOR CASES FOR THE SMOKE AND UO<sub>2</sub> TRANSPORT

No	Aerosol initial mass (kg)	Rel.	Density (kg/m <sup>3</sup> )	Aerosol Fraction*, **	
				Atmos.	Dep.
12	0.29 (s)** 0.1 (u)**	Cont.	11000.0	0.9221(s) 0.6186 (u)	0.0779(s) 0.3814 (u)
13	0.29 (s)** 0.1 (u)**	Cont.	800.0	0.9317 (s) 0.8283 (u)	0.0683(s) 0.1717 (u)
14	0.29 (s)** 0.1 (u)**	Puff	11000.0	0.9221 (s) 0.4884 (u)	0.0779 (s) 0.5116 (u)
15	0.29 (s)** 0.1 (u)**	Puff	800.0	0.9317 (s) 0.7197 (u)	0.0683 (s) 0.2803 (u)
16	0.29 (s)** 0.1 (u)**	Cont.	3407.0	0.9265 (s) 0.7197 (u)	0.0735(s) 0.2803 (u)
17	0.29 (s)** 0.1 (u)**	Puff	3407.0	0.9269 (s) 0.6003 (u)	0.0731(s) 0.3997 (u)

\*at the end 500 s simulation time

\*\*(s) = smoke, (u)=UO<sub>2</sub>

A typical DOE facility may have a corridor that connects to the environment through a doorway. If this doorway remains open, the aerosol may escape through the opening due to external or thermal effects inside the facility where the fire is located. Because FM21 does not model this opening, we assume both TR1 and TR2 as environmental volumes. As shown in TABLE 7, four cases were examined to study the effect of puff versus continuous release of UO<sub>2</sub>, and effect of the aerosol density. As

shown in this table, using a higher density decreases the release to the environment regardless of puff or continuous release. On the other hand, the puff release yields a lower environmental release due to the sudden surge of aerosol in a short time to allow more agglomeration to occur, which increases the deposition rate. As shown in FIGURE 23(a), there is an increase in the gas velocities in the doorways which are higher than that of Case 0 (see FIGURE 11(a)) due to the low constant temperature and pressure of the environment. Thus, these effects significantly influence the pressure drop across BR and CR due to a greater cooling effect.

**TABLE 7:** MELCOR CASES FOR THE SMOKE AND UO<sub>2</sub> TRANSPORT WITH TREATING TR1 AND TR2 AS ENVIRONMENT

No	Rel. ( $\rho$ , kg/m <sup>3</sup> )	Aerosol Fraction*,**			
		Atmos.** *	Dep.***	TR1 (UO <sub>2</sub> )	
18	Cont. (3407)	0.9746(s) 0.1754(u)	0.0254(s) 0.1710 (u)	0.3760	0.2766
19	Puff (3407)	0.9729 (s) 0.0164 (u)	0.0270 (s) 0.2638 (u)	0.3419	0.3779
20	Cont. (11000)	0.9712 (s) 0.0157 (u)	0.0286 (s) 0.2638 (u)	0.3399	0.2389
21	Puff (3407)	0.9712 (s) 0.0138 (u)	0.0286 (s) 0.3677 (u)	0.2994	0.3191

\*at the end 500 s simulation time

\*\*(s) = smoke, (u)=UO<sub>2</sub>

\*\*\*Fractional value of UO<sub>2</sub> in volumes other than in TR1 and TR2

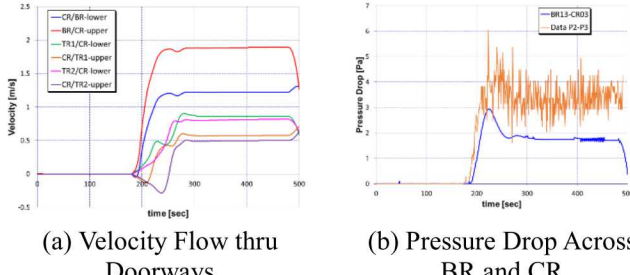


**FIGURE 23:** DOORWAY VELOCITIES AND PRESSURE DROP FOR CASE 18

## 6. CONCLUSION

This paper summarizes the validation work on MELCOR for modeling a multiroom fire with a corridor. This validation work demonstrates that MELCOR can be used for modeling a fire source term, even though it lacks a specialized hot gas layer model. Furthermore, the sensitivity studies provided insight on the effect of smoke aerosols and containment entrainment rates on ST. Results demonstrate that, despite MELCOR's current limitation of using single aerosol density, the density smearing technique is adequate to bound the situation where both lighter soot and heavier contaminant such as UO<sub>2</sub> exist in the same problem. In terms of aerosol entrainment rate effect on ST, results showed that puff release yields a lower ST than continuous rate entrainment.

## ACKNOWLEDGEMENTS

The authors would like to thank Sandia staff: K.C. Wagner, Christ Faucett, and Kyle Ross (former staff), and LANL staff: Cody Muchmore and Joshua Benson for assisting and reviewing this work and this paper. This work is supported by the Integrated Contractor Order (505767) from Triad National Security, LLC. Sandia National Laboratories is managed and operated by National Technology and Engineering Solutions of Sandia, LLC under DOE NNSA contract DE-NA0003525. Los Alamos National Laboratory is managed and operated by Triad National Security, LLC under DOE NNSA contract 89233218CNA000001. Los Alamos National Laboratory-Environmental Management is managed and operated by Newport News Nuclear BWXT (N3B), LLC under DOE contract 89303318CEM000007

## REFERENCES

- [1] <https://www.energy.gov/ehss/safety-software-quality-assurance-central-registry>
- [2] Humphries, L.L., et al., "MELCOR Computer Code Manuals, Vol. 1: Primer and Users' Guide, Version 2.2.9541 2017," SAND2017-0455 O, Sandia National Laboratories, 2017.
- [3] Peacock, R., et al., "CFAST-Consolidated Model of Fire Growth and Smoke Transport (Version 7), Volume 2: User's Guide, NIST Technical Note 1889v2," National Institute of Standards and Technology, 2019.
- [4] Louie, D., and Humphries, L., "NSRD-10: Leak Path Factor Guidance Using MELCOR," SAND2017-3200, Sandia National Laboratories, Albuquerque, NM, March 2017.
- [5] Peacock, et al, "CFAST-Consolidated Fire and Smoke Transport (Version 7) Volume 3: Verification and Validation Guide," National Institute of Standards and Technology, 2019.
- [6] Heskestad, G., et al., "Experimental Fires in Multiroom/Corridor Enclosures," FMRC J.I. 0J2N8.RU, NBS-GCR-86-502, Factory Mutual Research Corporation, Norwood, MA, October 1985.
- [7] [https://github.com/firemodels/exp/blob/master/FM\\_NB\\_Sfm21.csv](https://github.com/firemodels/exp/blob/master/FM_NB_Sfm21.csv).
- [8] Butler, et al., "Generation and Transport of Smoke Components," *Fire Technology*, 40, pg 149-176, 2004.
- [9] Mishima, J., et al., "Some Experimental Measurements of Airborne Uranium (Representing Plutonium) in Transportation Accidents," BNWL-1732, August 1973.
- [10] [https://github.com/firemodels/cfast/blob/master/Validation/FM\\_NBS/FM21.in](https://github.com/firemodels/cfast/blob/master/Validation/FM_NBS/FM21.in).
- [11] Hurley, Morgan, "SFPE Handbook of Fire Protection Engineering," 5th Edition. Springer, 2016.